Physica D 50 (1991) 311–320
North-Holland

Effect of noise and perturbations on limit cycle systems

Christian Kurrer and Klaus Schulten

Department of Physics and Beckman Institute, University of Illinois at Urbana-Champaign, 405 N. Mathews, Urbana, IL 61801, USA

Received 15 March 1990
Accepted 24 September 1990
Communicated by A.V. Holden

This paper demonstrates that the influence of noise and of external perturbations on a nonlinear oscillator can vary strongly along the limit cycle and upon transition from limit cycle to stationary point behaviour. For this purpose we consider the role of noise on the Bonhoeffer–van der Pol model in a range of control parameters where the model exhibits a limit cycle, but the parameters are close to values corresponding to a stable stationary point. Our analysis is based on the van Kampen approximation for solutions of the Fokker–Planck equation in the limit of weak noise. We investigate first separately the effect of noise on motion tangential and normal to the limit cycle. The key result is that noise induces diffusion-like spread along the limit cycle, but quasistationary behaviour normal to the limit cycle. We then describe the coupled motion and show that noise acting in the normal direction can strongly enhance diffusion along the limit cycle. We finally argue that the variability of the system's response to noise can be exploited in populations of nonlinear oscillators in that weak coupling can induce synchronization as long as the single oscillators operate in a regime close to the transition between oscillatory and excitatory modes.

1. Introduction: Nonlinear dynamical systems in biology

Many life processes depend on nonlinear controls. Examples are biochemical kinetics [1], biomolecular evolution [2], morphogenesis [3, 4], the circadian clock [5], and neural systems, e.g. a single nerve cell [6]. In some cases, the underlying nonlinear dynamical systems are well understood, for example in biochemical kinetics, in other cases attempts are being made to show that unknown control mechanisms can be modelled by rather simple nonlinear dynamics. In this paper we want to focus on biological systems and on corresponding models that exhibit excitable or oscillatory behaviour, mainly on the dynamics of a single neuron.

In groundbreaking work, Hodgkin and Huxley [6] proposed a set of four nonlinear differential equations (HH equations) to reproduce the action potential of a squid neuron. FitzHugh [7] proposed a transformation to reduce the four-dimensional HH equations to a two-dimensional set of equations. The equations arrived at are the so-called Bonhoeffer–van der Pol equations (BvP equations) based on earlier work by van der Pol [8] and Bonhoeffer [9]. The deterministic models (HH and BvP) were successful in reproducing the two states of a neuron, firing at a constant rate and silence. However, additional stochastic processes [10–14] need to be added to the BvP dynamics to account for a variable rate of firing that can vary continuously between silence, i.e. firing at a rate of 0 kHz, and firing at a rate of about 1 kHz.

In the following a description of stochastic dynamic systems suggested by van Kampen [15] will be applied to analyze the BvP model in the

proximity of a neuron's limit cycle. We will demonstrate that local properties of the dynamics near the limit cycle have a great impact on the way that the corresponding systems can be influenced by random noise or by interactions with other oscillating systems.

In section 2 the Fokker–Planck equation for a neuron subject to stochastic forces and the van Kampen solution in the limit of small fluctuations are introduced. In section 3 the van Kampen solution is analyzed. In section 4 implications of our results for large systems of interacting nonlinear oscillators, e.g. neurons in neural networks, are discussed.

2. Mathematical framework

2.1. Deterministic systems

Our investigations will be based on a system described by the nonlinear differential equations (BvP equations)

$$\begin{aligned}\dot{x}_1 &= F_1(x_1, x_2)\\ &= c\left(x_1 - x_1^3/3 + x_2 + z\right),\\ \dot{x}_2 &= F_2(x_1, x_2)\\ &= (a - x_1 - bx_2)/c\end{aligned} \tag{1}$$

introduced by FitzHugh [7]. In this model x_1 represents essentially the voltage of a neuron and x_2 can be identified with the conductivity of the potassium channels of the neural membrane. z is an essential control parameter of the system and in the range $-0.6 < z < 2.0$ represents physiologically possible excitation of the system due to transmembrane currents [7, 14]. The BvP equations provide a prototype for two-dimensional nonlinear dynamical systems that show excitable and oscillatory behaviour. We assume the parameters $a = 0.7$, $b = 0.8$, $c = 3.0$, which are widely used in the literature [7, 14]. Phase plane analysis [7, 14] of the stationary point of eq. (1) shows that in the range $-0.6 < z < -0.3465$ the system has an unstable stationary point and exhibits limit cycle behaviour; in the range $-0.3465 < z < 2.0$ the system has a stable stationary point. In the following, we will use a value of $z = -0.4$, for which the stationary point is unstable such that all trajectories eventually lead into a limit cycle.

2.2. Stochastic systems

In order to show that the limit cycle of the BvP model exhibits different stability characteristics along different sections one can apply various perturbations during a revolution of the system around the limit cycle and monitor the response. A more systematic approach for such investigation is to apply noise to the system and to investigate the dynamics of a large ensemble of BvP oscillators. For the sake of simplicity we apply isotropic Gaussian white noise $\eta(t)$, characterized by

$$\begin{aligned}&\langle \eta(t) \rangle = 0,\\ &\langle \eta(t_1)\eta(t_2) \rangle = \beta^{-1}\delta(t_1 - t_2).\end{aligned} \tag{2}$$

Such noise added to the BvP equations yields the stochastic differential equations

$$\begin{aligned}\dot{x}_1 &= F_1(x_1, x_2) + \eta_1(t),\\ \dot{x}_2 &= F_2(x_1, x_2) + \eta_2(t).\end{aligned} \tag{3}$$

An ensemble of systems governed by eqs. (3) is described by the density $p(\boldsymbol{x}, t)$ which gives the probability to find a system at position $\boldsymbol{x} = (x_1, x_2)^{\mathrm{T}}$ at time t. The evolution of $p(\boldsymbol{x}, t)$ is governed by the Fokker–Planck equation [16]

$$\begin{aligned}&\partial_t p(\boldsymbol{x}, t)\\ &= \left(-\sum_i \partial_i F_i(\boldsymbol{x}) + \tfrac{1}{2}\beta^{-1} \sum_i \partial_i^2 \right) p(\boldsymbol{x}, t).\end{aligned} \tag{4}$$

We want to consider the solution of eq. (4) for

the initial condition [#1]

$$p(x, t=0) = \delta(x - x_0). \tag{5}$$

Van Kampen [15] analyzed solutions of (4), (5) in the limit of weak noise. In this limit, $p(x,t)$ should be peaked around the deterministic solution x_{det} of eqs. (1). Van Kampen [15] proposed to expand the Fokker–Planck equation in terms of deviations from the deterministic solution, scaled by the square root of the noise amplitude β defined in eq. (2)

$$y(t) = \beta^{1/2}[x - x_{\mathrm{det}}(t)]. \tag{6}$$

The scaling factor $\beta^{1/2}$ in eq. (6) allows to eliminate the explicit occurrence of β in the Fokker–Planck equation. Replacing the force field $F(x)$ by

$$F(x) = F(x_{\mathrm{det}}) + \left(\frac{\partial F}{\partial x}\right)_{x_{\mathrm{det}}} \cdot \beta^{-1/2} y \tag{7}$$

and, thus, omitting terms of higher order in $\beta^{-1/2}$, eq. (4) can be written in terms of the new coordinates $y(t)$ as

$$\partial_t p(y,t) = -\sum_{i,j} A_{ij}(t) \frac{\partial}{\partial y_i} y_j p(y,t) + \frac{1}{2} \sum_{i,j} B_{ij} \frac{\partial^2}{\partial y_i \partial y_j} p(y,t), \tag{8}$$

where

$$A_{ij}(t) = \left.\frac{\partial F_i}{\partial y_j}\right|_{x_{\mathrm{det}}(t)}, \tag{9}$$

$$B_{ij} = \delta_{ij}. \tag{10}$$

The amplitude β of the noise does no longer appear in eq. (8) since it has been eliminated by the substitution described in eq. (6). In fact, noise will be represented by a constant term (eq. (10)) independent of the actual amplitude of the noise.

The solution of the Fokker–Planck equation (8) according to ref. [15] is given by a Gaussian probability distribution,

$$p(y,t) = \frac{1}{2\pi\sqrt{\mathrm{Det}\,\Xi}} \exp\left(-\tfrac{1}{2} y^{\mathrm{T}} \cdot \Xi^{-1} \cdot y\right), \tag{11}$$

with $\Xi_{ij}(t) = \langle y_i(t)\, y_j(t) \rangle$. The matrix $\Xi(t)$ describes the second moments of the Gaussian probability distribution, i.e., size and orientation of the distribution in phase space. The overall width of the distribution $p(y,t)$ is

$$\sigma = \sqrt{\mathrm{Tr}(\Xi)}\,. \tag{12}$$

$\Xi(t)$, together with the position of the deterministic solution $x_{\mathrm{det}}(t)$ governed by eq. (1), provides a complete description of the probability distribution under the approximation made in eq. (7). $\Xi(t)$ is determined by the equation of motion [15]

$$\dot{\Xi} = \mathbf{A}(t)\Xi + \Xi\mathbf{A}^{\mathrm{T}}(t) + \mathbf{B} \tag{13}$$

and by the initial conditions $\Xi_{ij}(t=0) = 0$ for $i, j = 1, 2$, which follows from eq. (5). The elements of $\mathbf{A}(t)$, defined in eq. (9), take on positive as well as negative values and describe the expansion, contraction and rotation of the probability distribution. The elements of $\mathbf{B}$, defined in eq. (10), are constant and positive and describe a diffusive broadening of the distribution.

The description outlined is valid as long as the linearization introduced in eq. (7) holds, i.e. as long as the distribution extends over a small range. In the long time limit, this approximation does no longer apply. The distribution eventually will reach a stationary state in which it is smeared out over the whole limit cycle [17].

[#1] Throughout this paper, we use the value of $x_0 = (x_1, x_2) = (1.11, -0.32)$, which lies on the limit cycle in the proximity of the stationary point, as starting point for any numerical calculations.

3. Van Kampen analysis of the effect of noise on the BvP limit cycle

In this section we will investigate the effect of noise on the limit cycle of a BvP system. For this purpose we will assume first that the motion along the limit cycle and normal to the limit cycle are uncoupled, and that noise affects these motions separately. The effect of noise is easier to understand since the corresponding one-dimensional stochastic dynamical systems can be analyzed without resorting to numerical solutions. We will then present the solution of eq. (13) for coupled tangential and normal motion along the limit cycle.

3.1. *Effect of noise in direction along the limit cycle*

For the analysis presented in sections 3.1, 3.2 we transform from $y_1(t)$, $y_2(t)$ coordinates to coordinates $y_l(t)$ tangential and $y_n(t)$ normal to the limit cycle at the position $x_{det}(t)$ of the deterministic motion. In such a coordinate representation eq. (13) reads

$$\frac{d}{dt}\begin{pmatrix}\xi_{ll} & \xi_{ln}\\ \xi_{nl} & \xi_{nn}\end{pmatrix} = \begin{pmatrix}a_{ll} & a_{ln}\\ a_{nl} & a_{nn}\end{pmatrix}\begin{pmatrix}\xi_{ll} & \xi_{ln}\\ \xi_{nl} & \xi_{nn}\end{pmatrix} + \begin{pmatrix}\xi_{ll} & \xi_{ln}\\ \xi_{nl} & \xi_{nn}\end{pmatrix}\begin{pmatrix}a_{ll} & a_{nl}\\ a_{ln} & a_{nn}\end{pmatrix} + \begin{pmatrix}b & 0\\ 0 & b\end{pmatrix}. \qquad (14)$$

Here we have defined $\Xi_{ll} = \xi_{ll}$, $\Xi_{ln} = \xi_{ln}$, etc. and $A_{ll} = a_{ll}$, $A_{ln} = a_{ln}$, etc. These equations neglect terms due to the time dependence of the transformation. Since the equations will serve only for a qualitative analysis of the behaviour of the diagonal elements of $\Xi(t)$ the neglect of 'Coriolis-type' terms is not essential. The value of b is 1, if the system is subjected to noise, and 0 in the absence of noise.

First, we want to consider *separately* the dynamics in the two directions normal and tangential to the limit cycle. In the direction *tangential* to the limit cycle, eq. (14) reduces to

$$\dot{\xi}_{ll} = 2a_{ll}\xi_{ll} + b, \qquad (15)$$

which describes the expansion and contraction of the longitudinal distribution during its motion along the limit cycle. The solution of (15) yields the width σ_l of the distribution when motion is confined to the limit cycle

$$\sigma_l = \sqrt{\xi_{ll}}\,. \qquad (16)$$

The solution is determined through the values of $a_{ll} = \partial F_l/\partial y_l$ evaluated at points $x_{det}(t)$ along the limit cycle. The index l refers to the direction tangential to the limit cycle. $t \in [0, T[$ denotes the time which serves here as a parameter to define the locations on the limit cycle, T being the period of the limit cycle. We will also allow t values larger than T which correspond then to more than one revolution around the limit cycle.

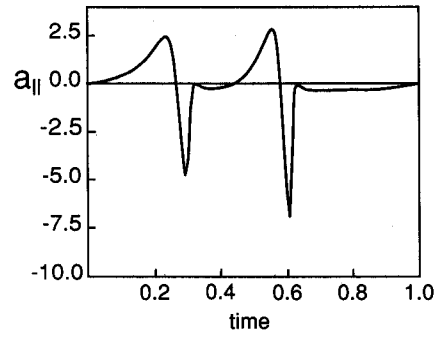

Fig. 1. Derivative a_{ll} of the longitudinal force F_l in the direction tangential to the limit cycle during one revolution along the limit cycle. The time axis is labeled in units of the limit cycle period T.

Fig. 1 presents the values of a_{ll} for one revolution around the limit cycle. The variation of a_{ll} demonstrates clearly that the dynamics along the limit cycle is not uniform. One can discern regions with positive a_{ll} (expansion of width σ_l) and with negative a_{ll} (contraction of width σ_l). The question arises which of the contributions of a_{ll}, i.e. the positive or the negative ones, are more

prevailing. To answer this question we consider motion around the limit cycle first in case of a system *without noise*, i.e. for the case $b = 0$ in (15). Integration of (15) yields

$$\xi_{ll}(t+T) = \xi_{ll}(t) \exp\left(2\int_t^{t+T} a_{ll}(t')\,dt'\right). \tag{17}$$

To evaluate the integral in the exponent we will introduce the path element ds along the limit cycle which is related to dt by $dt = F_l^{-1}\,ds$. With the identities

$$a_{ll}(t)\,dt = (dF_l/ds)(1/F_l)\,ds = d(\log F_l)$$

one obtains

$$\exp\left(2\int_{t_1}^{t_2} a_{ll}(t')\,dt'\right) = \left(\frac{F_l(t_1)}{F_l(t_2)}\right)^2. \tag{18}$$

For $t_2 = t_1 + T$ this expression is unity and, hence, $\xi_{ll}(t+T) = \xi_{ll}(t)$. In the noise-free case this cyclic property of $\xi_{ll}(t)$, of course, is to be expected. The derivation shows that the contribution of a_{ll} in eq. (15) along a complete revolution around the limit cycle balances contracting and expanding contributions. This implies, however, that for a system subjected to noise over one or over several revolutions around the limit cycle the noise term will dominate $\xi_{ll}(t)$ and will induce a diffusion-type broadening.

To study such broadening we consider now the integration of (15) for nonvanishing b. Integration of (15) yields

$$\xi_{ll}(t_0+t) = \left[\xi_{ll}(t_0) + b\int_{t_0}^{t_0+t} dt' \exp\left(-2\int_{t_0}^{t'} dt''\, a_{ll}(t'')\right)\right] \times \exp\left(2\int_{t_0}^{t_0+t} dt'\, a_{ll}(t')\right). \tag{19}$$

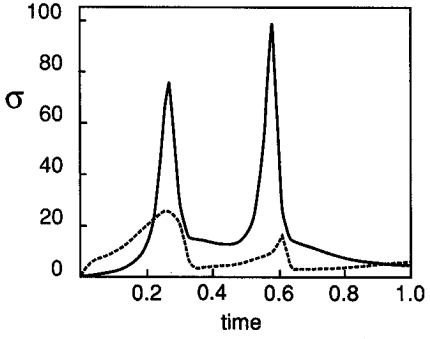

Fig. 2. Longitudinal and normal widths σ_l (—) and σ_n (· · ·) of the probability distribution during one limit cycle period. The time axis is labeled in units of the limit cycle period T. σ_n has been multiplied by a factor 10 to be visible on the same scale.

The resulting width σ_l over one revolution around the limit cycle is presented in fig. 2. One can recognize two segments along the limit cycle during which the width increases and decreases. The beginning of these two segments coincide with those parts of the limit cycle for which a_{ll} assumes positive values. One also discerns in fig. 2 that the presence of noise leads to a small, but significant residual width after the revolution around the limit cycle is completed. To demonstrate how this residual width develops over a longer time period we present in fig. 3 the width σ_l over 20 revolutions around the limit cycle. The results show an increase of σ_l proportional to $\sqrt{t}$. This diffusion-like behaviour can be derived from the solution (19) taken for $t = NT$. By means of

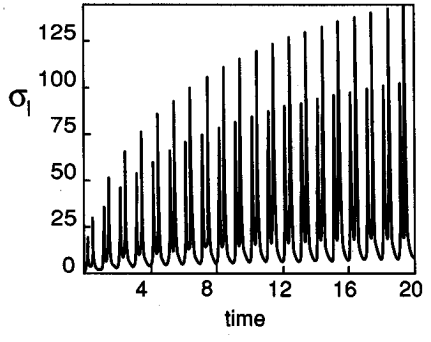

Fig. 3. Longitudinal width $\sigma_l = \xi_{ll}^{1/2}$ of the probability distribution during 20 limit cycle periods.

(18) we obtain

$$\xi_{ll}(t_0+NT) = \xi_{ll}(t) + b\sum_{j=0}^{N-1}\int_{t_0+jT}^{t_0+(j+1)T} dt\left(\frac{F_l(t_0+jT)}{F_l(t)}\right)^2. \tag{20}$$

Since $F_l(t)$ is cyclic, i.e. $F_l(t+T)=F_l(t)$, the contributions in the sum are all identical and the final expression for $\xi_{ll}(t_0+NT)$ is

$$\xi_{ll}(t_0+NT) = \xi_{ll}(t) + NTbF_l^2(t_0)\left\langle F_l^{-2}(t)\right\rangle_T. \tag{21}$$

In this expression $\langle F_l^{-2}(t)\rangle_T$ denotes a *time* average which is equal to the *space* average $(L/T)\langle F_l^{-3}(s)\rangle_L$ where L is the length of the limit cycle. From eq. (21) follows

$$\sigma_l(t_0+NT) = \sqrt{\sigma_l^2(t_0) + NTbF_l^2(t_0)\left\langle F_l^{-2}(t)\right\rangle_T} \tag{22}$$

which clearly exhibits the $\sqrt{t}$ dependence ($t=NT$) seen in fig. 3.

3.2. *Effect of noise in direction normal to the limit cycle*

In the direction *normal* to the limit cycle, eq. (14) reduces to

$$\dot{\xi}_{nn} = 2a_{nn}\xi_{nn} + b. \tag{23}$$

Solution of this equation yields the width of the distribution normal to the limit cycle defined as $\sigma_n = \sqrt{\xi_{nn}}$. Fig. 4 presents the values of a_{nn} during one revolution around the limit cycle. a_{nn} is found to be negative over most, but not all parts of the limit cycle. Negative values of a_{nn} correspond to contraction of the normal distribution, i.e. trajectories near segments of the limit cycle with $a_{nn}<0$ are attracted to the limit cycle. The dominance of negative a_{nn} values implies that the average $T^{-1}\int_t^{t+T} dt'\, a_{nn}(t')$ is negative and that

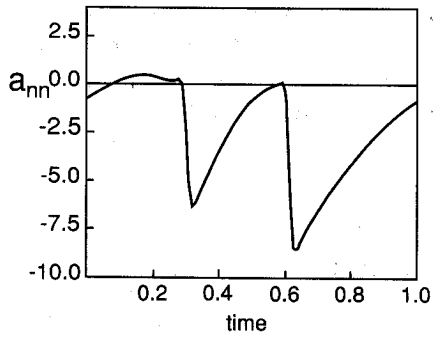

Fig. 4. Derivative a_{nn} of the normal force F_n in the direction orthogonal to the limit cycle during one revolution along the limit cycle. The time axis is labeled in units of the limit cycle period T.

the limit cycle is stable against perturbations in the normal direction. This stability, in fact, is so strong, that contraction due to a_{nn} and diffusive broadening due to b induces the distribution to follow (approximately) adiabatically the equilibrium width

$$\sigma_n(t) \sim \sqrt{\frac{b}{-2a_{nn}(x_{det}(t))}} \tag{24}$$

along those segments of the limit cycle where a_{nn} is negative. This behaviour is clearly reflected in the long-time behaviour of $\sigma_n(t)$ presented in fig. 5; the width $\sigma_n(t)$, after a brief transient behaviour during the first limit cycle period, shows a cyclic behaviour at later times, i.e. $\sigma_n(t)$ averaged over consecutive limit cycles remains constant.

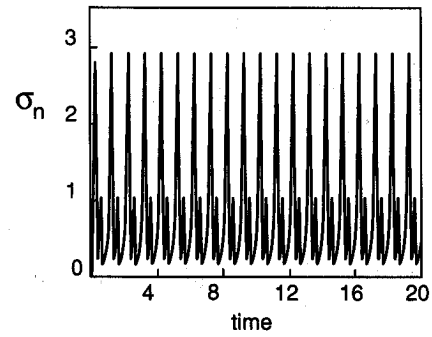

Fig. 5. Normal width $\sigma_n = \xi_{nn}^{1/2}$ of the probability distribution during 20 limit cycle periods.

The increase and decrease of $\sigma_n(t)$ according to eq. (24) reflects the change of the local a_{nn} values along the limit cycle. During the two short segments where a_{nn} is positive, the width briefly expands exponentially, to be contracted again along segments with $a_{nn} < 0$.

The variable behaviour of σ_l and σ_n along a limit cycle revolution demonstrates strikingly that the stability of the limit cycle against noise and other perturbations varies along its path. The occurrence of exponential growth and peaks in the width σ_n of the distribution at certain points of the limit cycle implies that the Brownian trajectories at these points will show great variability in their deviation from the limit cycle to either side. Small disturbances at the beginning of an exponential growth period ($a_{nn} > 0$) have a large effect on the trajectories. The strong variation of σ_l along the limit cycle and its diffusive behaviour on a time scale of many limit cycle periods implies that the phase of the system along the limit cycle can be affected through noise, and that the effect of noise depends much on the position on the limit cycle where it acts on the system.

We want to demonstrate in the next subsection that the effects of noise in the direction tangential and normal to the limit cycle are actually strongly coupled such that the behaviour of both σ_l and σ_n is most relevant for judging how noise or external perturbations will influence an oscillating BvP system.

3.3. *Effect of noise on coupled tangential and normal motion along the limit cycle*

Up to now we treated the two directions of diffusion normal and tangential to the limit cycle separately. We now want to focus on effects that arise from the coupling of normal and tangential diffusion in eq. (13). This coupling is effected through the nondiagonal elements of the **A** matrix in eq. (13), which had neither been considered in eq. (15) nor in eq. (23). We will deal with eq. (23) in the y_1, y_2 representation, i.e. the error

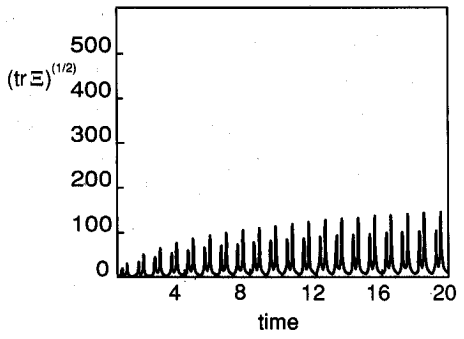

Fig. 6. Overall width $(\mathrm{Tr}\,\Xi)^{1/2}$ of the probability distribution during 20 limit cycle periods without coupling between longitudinal and normal diffusion, i.e. eqs. (15) and (23) were used to evaluate the diagonal elements of Ξ separately.

from the time dependence of the $y_1, y_2 \to y_l, y_n$ transformation does not arise.

It is intuitively clear that if the phase point is disturbed in a direction normal to the limit cycle, a trajectory results that eventually reaches the limit cycle again, but its phase point, in general, is not found at exactly the same position as another phase point that started at the same position on the limit cycle but was not disturbed. Because of this difference of positions between the two phase points, fluctuating forces normal to the limit cycle contribute to diffusive broadening in the longitudinal direction of the limit cycle and, as will be shown shortly, can enhance significantly the effect of noise on the phase along the limit cycle.

Figs. 6 and 7 compare the evolution of the overall width σ of the distribution defined in eq. (12) during propagation over 20 limit cycle periods with and without coupling of longitudinal and normal motion. The results presented in fig. 6 have been obtained by integrating separately eq. (15) and eq. (23) and then evaluating $\sigma(t) = \sqrt{\xi_{ll} + \xi_{nn}}$. The results presented in fig. 7 have been obtained by integration of the matrix differential equation (13) and evaluation of $\sigma(t)$ according to the definition (12). Comparison of figs. 6 and 7 shows that the coupling of longitudinal and normal motion increases the overall width $\sqrt{\mathrm{Tr}\,\Xi}$ by a factor of approximately four over the width $\sigma(t) = \sqrt{\xi_{ll} + \xi_{nn}}$ of the uncoupled motion.

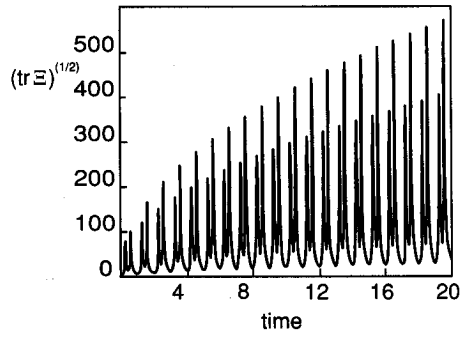

Fig. 7. Overall width $(\mathrm{Tr}\,\Xi)^{1/2}$ of the probability distribution during 20 limit cycle periods with coupling between longitudinal and normal diffusion, i.e. eq. (13) was integrated to obtain the matrix Ξ.

Further analysis of the results showed that this increase is mainly due to an increase of the tangential component of $\Xi(t)$. The results in figs. 6 and 7 demonstrate that noise acting on the motion normal to the limit cycle contributes strongly to phase diffusion.

4. Concluding remarks and outlook

We have demonstrated above that the influence of noise and, hence, of any other external perturbation on a nonlinear oscillator described by the BvP equations varies strongly along the limit cycle. For this purpose we have employed the van Kampen approximation to describe the width of a distribution circling the limit cycle. The van Kampen approximation characterizes the stability of nonlinear oscillators against phase diffusion and deviations from the limit cycle. Although the approximation becomes exact only in the limit of weak noise, it should often also yield information about responses which are characterized by large deviations from the unperturbed oscillator motion. This situation is similar to the case of the celebrated linear stability analysis for nonlinear dynamical systems which applies strictly only in a small neighborhood of a fixpoint but nevertheless often allows conclusions about global dynamics patterns.

The properties of single nonlinear oscillators subject to external perturbations are significant in view of the interesting behaviour of systems of coupled nonlinear oscillators. Such systems can be characterized often as attractor networks, in that sets of initial conditions can be considered basins of attraction which lead the network to a small number of final states, the most prominent among them the state in which the oscillators are all synchronized. The results of our paper should be pertinent to neural networks viewed as coupled nonlinear oscillators. We like to argue that in such systems one has to take account of the structure of the limit cycle of neurons. The latter operate often in a regime of control parameters near the transition between oscillatory and stationary behaviour: in the oscillator regime neurons are sufficiently and continuously excited that they exhibit a constant rate of firing, in the stable stationary state regime neurons behave as threshold units which fire only once after a sufficient deviation from the stationary point.

We like to explain now to what extent a limit cycle of a BvP neuron becomes more *structurally unstable* as the control parameter z approaches the critical value $z_c = -0.3465$ at which the transition to a stable stationary point behaviour takes place. *Structural instability* of the system for $z \simeq z_c, z < z_c$ implies that a neuron reacts sensitively to small perturbations by shifting its firing phase considerably. This sensitivity, observed both for fluctuations tangential and fluctuations normal to the limit cycle, can be readily explained. As z approaches z_c, the stationary point moves closer and closer to the limit cycle. The motion of the phase point on the limit cycle near the stationary point will slow down, whereas the motion in regions of the limit cycle further away from the stationary point is affected only insignificantly. The phase point, therefore, spends more and more of the limit cycle period in a relatively small segment of the limit cycle, i.e. in proximity to the stationary point. By perturbing the phase point in that region of the limit cycle, one can shift its phase by a large amount.

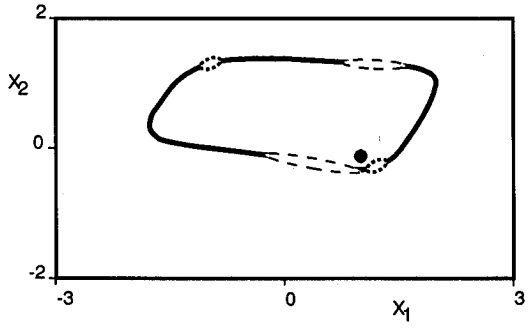

Fig. 8. Limit cycle (—) and stationary point (•) in the phase plane of the BvP model for $z = -0.4$. On the limit cycle, the regions most sensitive to tangential (· · ·) and normal (– – –) perturbation have been encircled.

In the direction normal to the limit cycle, perturbations also have an increasing impact on the phase of the limit cycle. The reason is that $a_{nn} = \partial F_n/\partial x_n$, which, as shown earlier, is a measure of the local stability of the limit cycle, generally increases in the proximity of the stationary point as the stationary point approaches the limit cycle. Even small perturbations normal to the limit cycle can then lead to large deviations of the trajectories of the phase point away from the limit cycle and eventually translate into a large phase shift. (For an extension of the definition of phase to regions in the proximity of the limit cycle, see e.g. ref. [18].)

Fig. 8 illustrates the sensitive areas on the limit cycle. It shows areas, characterized by a local minimum of σ_1, that are sensitive to longitudinal perturbations, and areas, characterized by positive a_{nn}, that are sensitive to normal perturbations.

We like to propose that structural instability plays an important role in the synchronization of nonlinear oscillators. Many experimental studies suggested that fast synchronization of neurons in the visual [19, 20] and olfactory [21] cortex is a key element in the process of feature detection. Most former theoretical investigations into the self-synchronization of nonlinear oscillators [18, 22–24] assumed structurally stable limit cycles as components of a large ensemble; such oscillators, however, allow only gradual synchronization. Furthermore these investigations focused on the question to what extent the degree of synchronization of a population of oscillators can be controlled through the strength of the inter-oscillator coupling. The investigations would imply that neural systems achieve synchronization through variation of synaptic interactions. However, experimental evidence for short time variation of the synaptic strength of neurons is scarce and disputed. We like to suggest that the transition to a synchronized state of neurons is not mediated by varying the strength of synaptic connections, but rather by changing the susceptibility to synchronization of the cells by effectively altering the z value, which in the BvP model represents the "excitation" of the neuron, nearer to its critical value. Such change can be achieved through systematic input of neurons, e.g. through input from the retina to a subset of neurons in the optical cortex. If neurons representing a particular feature, e.g. optical flow into a certain direction and of a particular magnitude, are excited in an area of the image corresponding to an object, they may receive sufficient excitation to be sensitized such that lateral interactions specific for the subpopulation of neurons coding the respective feature suffice to synchronize firing. Such linking of neurons may, for example, explain filling-in capabilities or figure–ground separation.

The importance of the above outlined structural instability for the fast synchronization of neurons is supported by the observation that neurons in the olfactory and visual cortex alternate between excitable and self-oscillatory behaviour and, thus, seem to operate in the dynamical regime where the z value in the BvP model is close to its critical value.

Acknowledgements

This work has been supported by the University of Illinois at Urbana-Champaign and by a grant of the National Science Foundation DMR

89-20538 (through the Materials Research Laboratory of the University of Illinois).

Note added in proof

Since the submission of this article various groups have reported investigations on the capacity for figure ground separation through synchronized firing, see for example ref. [25].

References

[1] L. Michaelis and L.M. Menten, Biochem. Z. 49 (1913) 79.
[2] M. Eigen and P. Schuster, Naturwissenschaften 64 (1977) 541.
[3] A. Gierer and H. Meinhardt, Kybernetik 12 (1972) 30.
[4] H. Meinhardt, Models of Biological Pattern Formation (Academic Press, London, 1982).
[5] A.T. Winfree, The Geometry of Time (Springer, Berlin, 1980).
[6] A.L. Hodgkin and A.F. Huxley, J. Physiol. London 117 (1952) 500.
[7] R. FitzHugh, Biophys. J. 1 (1961) 445.
[8] B. van der Pol, Philos. Mag. 2 (1926) 978.
[9] K.F. Bonhoeffer, Naturwissenschaften 40 (1953) 301.
[10] H. Lecar and R. Nossal, Biophys. J. 11 (1971) 1048.
[11] H. Lecar and R. Nossal, Biophys. J. 11 (1971) 1064.
[12] A.V. Holden, Models of Stochastic Activity of Neurons, Lecture Notes in Biomathematics, Vol. 12 (Springer, Berlin, 1976).
[13] L.M. Ricciardi, in: Competition and Cooperation in Neural Nets, ed. S. Levin (Springer, Berlin, 1982).
[14] H. Treutlein and K. Schulten, Ber. Bunsenges. Phys. Chem. 89 (1985) 710–718.
[15] N.G. van Kampen, Stochastic Processes in Physics and Chemistry (North-Holland, Amsterdam, 1981).
[16] H. Risken, The Fokker–Planck Equation (Springer, Berlin, 1984).
[17] H. Treutlein and K. Schulten, Eur. Biophys. J. 13 (1986) 355–365.
[18] Y. Kuramoto, Physica A 106 (1981) 128–143.
[19] R. Eckhorn, H.J. Reitboeck, M. Arndt and P. Dicke, in: Proceedings of the IJCNN, Washington, D.C., Vol. 1 (June 1989) pp. 723–730, IEEE Catalog No. 89CH2765-6.
[20] C.M. Gray, P. König, A.K. Engel and W. Singer, Nature 338 (1989) 334–337.
[21] C.S. Skarda and W.J. Freeman, Behav. Brain Sci. 10 (1987) 161–195.
[22] Y. Kuramoto and I. Nishikawa, J. Stat. Phys. 49 (1987) 569.
[23] L.L. Bonilla, J.M. Casado and M. Morillo, J. Stat. Phys. 48 (1987) 571.
[24] S.H. Strogatz and R.E. Mirollo, Physica D 31 (1988) 143–168.
[25] H. Sompolinsky, D. Golomb, and D. Kleinfeld, PNAS 87 (1990) 7200–7204;
Ch. Kurrer, B. Nieswand and K. Schulten, in: Self-Organization, Emergent Properties and Learning, ed. A. Babloyantz (Plenum Press, New York, 1991).